

# Characteristics of Gas Seepage and Pore Structure Response in CO<sub>2</sub>-ECBM Process of Low Permeability Coal Seam

Junlin Liu\*, Kun Zhang and Huihu Liu

School of Earth and Environment, Anhui University of Technology, Huainan, China

**Abstract.** CO<sub>2</sub>-ECBM is a method of enhanced coalbed methane extraction followed by cutting greenhouse gas emissions and new energy development. In order to reveal the characteristics of gas flow in porous media and the pore structure response characteristics of coal rocks, the experiments were carried out to simulate the process of CO<sub>2</sub> displacement of N<sub>2</sub> at a buried depth of 900 m, including monitoring the changes in gas permeability and strain of coal samples along with a comparison of the pore structure of low-temperature liquid nitrogen adsorption on coal samples both before and after displacement were both done. The findings of the experiment are listed below. The N<sub>2</sub> permeability of the LiuZhuang sample ranges from 0.0008mD to 0.0014mD, whereas the permeability of QiDong is around 0.0003mD. With an increase in gas injection duration and an expansion of the coal matrix for N<sub>2</sub> adsorption, the permeability steadily decreases. The efficient stress compression of the coal pore fracture structure during sample preparation and testing avoids the visible fracture region, which results in poor permeability. The displacement stages of CO<sub>2</sub> can be divided into three phases. Free nitrogen flows from the end of the position and the permeability diminishes during the phase of free nitrogen. When CO<sub>2</sub> is introduced into the penetration stage, the permeability tends to rise, however when there is no penetration, the permeability test values are frequently low. During the CO<sub>2</sub> steady displacement phase, gas permeability gradually declines. Axial and radial strains are progressively raised during the initial stage of the CO<sub>2</sub> injection whereas they are gradually reduced during the initial stage of the N<sub>2</sub> injection. While CO<sub>2</sub> is continuously supplied through the coal body stage, there are modest axial and radial strain changes. The axial and radial stresses are stabilized by the CO<sub>2</sub> displacement. The overall pore volume of the coal significantly rises following the displacement. The increase part of the pore volume is primarily focused on the pore of absorption and filling (aperture < 10nm), whereas the decreased part is mainly concentrated in the diffusion pore of the Fick type and the permeability part (aperture > 50nm). The increased in pore volume ratio surface area is centered mostly in the fill pore region (aperture 10 nm) and is four times greater than it was before the displacement. The CO<sub>2</sub> injection exerts an expansion impact on the adsorption-filled and diffusion pores during the CO<sub>2</sub>-ECBM process, whereas the compression effect on the percolation pores results in a reduction in permeability.

**Keywords:** CO<sub>2</sub>-ECBM, characteristics of gas flow in porous media, characteristics of pore structure response.

## 1. Introduction

The low-carbon economy has taken on the role of the trend of the sustainable and healthy growth of human civilization in light of the growing global greenhouse effect and the harm to the natural environment. Coal has played a significant role in the energy structure of China, which accounts for up to 70% of total energy consumption. Therefore, coal forms the bulk of the energy structure of China. However, compared to clean energy like natural gas, coal is less efficient to burn and more polluting. As a method of enhanced coalbed methane extraction followed by greenhouse gas emissions and new energy development, CO<sub>2</sub>-ECBM is in line with the new strategy

for energy security in China in light of the new alterations in energy supply and demand patterns as well as the new trends in international energy development[1]. CO<sub>2</sub>[2], N<sub>2</sub>[3], or a mixture of the two gases[4] are the gases that are typically employed in the ECBM process. Instead of CH<sub>4</sub>, CO<sub>2</sub> is initially adsorbed when the coal seam is absorbed[5]. Hence, the injected CO<sub>2</sub> is more simply adsorbed by the coal seam. N<sub>2</sub> is less effective than CO<sub>2</sub> in coal seam displacement, according to research by Jiang et al. Although N<sub>2</sub> can promote coal seam permeability, CO<sub>2</sub> injection causes a reduction in coal seam permeability[6]. With the application of modified triaxial loading rigs, Liu et al. discovered that the injection of CO<sub>2</sub> into the coal seam dramatically enhanced the

\* Corresponding author: 603093502@qq.com

expansion of the coal substrate, resulting in a decrease in permeability[7].

Most researchers have used physical simulation studies to analyze the features of the fluctuation of gas permeability in coal samples that have been injected with gas. As CO<sub>2</sub> displaces CH<sub>4</sub>, Li et al. analyzed the pattern of variation in coal seam permeability and discovered that CO<sub>2</sub> adsorption rises with falling pore pressure and falls with rising sealing pressure[8]. The change in coal permeability varies with the change in pore pressure and surrounding pressure throughout the process of displacing methane with CO<sub>2</sub>[9]. Non-isothermal CO<sub>2</sub> gas flow in porous media experiments were conducted by Wu et al. under the influence of thermodynamics. According to the study, pore pressure and CO<sub>2</sub> and CH<sub>4</sub> permeability are positively associated and the temperature has a negative exponential association with volume stress change[10]. In the gas permeability-stress coupling experiment of coal under the heat flow field, it was discovered that under the same pressure conditions, CH<sub>4</sub> displayed a strong permeability at high temperatures. As effective stress increases, permeability decreases[11–12]. Yin used a three-axis experimental setup to investigate the impact of CO<sub>2</sub> injection pressure on the desorption of CH<sub>4</sub> and to examine variations in gas concentration and CH<sub>4</sub>/CO<sub>2</sub> exit flow. According to the experimental findings, CH<sub>4</sub> generation efficiency decreases with increasing CO<sub>2</sub> injection pressure[13]. By using a gas-containing coal thermofluid-solid coupled triaxial servo seepage device to conduct experiments on the CO<sub>2</sub> gas flow in porous media characteristics in coal seams under various pressure conditions, Xu et al. discovered that the higher the ambient pressure, the slower the CO<sub>2</sub> permeation rate under the same axial pressure condition. The higher the axial pressure, the lower the rate of CO<sub>2</sub> infiltration under the same circumferential pressure. The stress sensitivity coefficient steadily declines with increasing stress under various axial and circumferential pressure settings, i.e., the greater the stress, the less sensitive the coal sample permeability rate is to stress[14]. In order to track changes in gas concentration and pore pressure, Wang et al. employed rectangular coal samples with dimensions of 300\*50\*50 mm and discovered that the injection of CO<sub>2</sub> might considerably increase the recovery of CH<sub>4</sub>. The breakthrough time of the injected gas is nonetheless shorter the greater the injection pressure<sup>[15]</sup>. Previous studies have demonstrated that factors including temperature, pressure, adsorbed gas, varying coal ranks, and water saturation all have an impact on how much CO<sub>2</sub> is displaced and absorbed[16–17]. However, the relevant alterations in stress-strain conditions, adsorption/desorption and permeability need to be further investigated[18-20].

We have utilized an experimental device to model the displacement of CH<sub>4</sub> by CO<sub>2</sub> under conditions of a coal reservoir in light of the aforementioned research state. The innovation of this paper lies in the following three aspects. Firstly, the experimental temperature and pressure settings are set up in accordance with the ground temperature and recurrence pressure gradient of the coal seam, which is the closest representation of the genuine coal reservoir. Secondly, the entire experiment—from the

CO<sub>2</sub> repulsion process to the CH<sub>4</sub> adsorption process—is fully and dynamically monitored, and the gas flow rate is tracked with the strain on the coal. Thirdly, analysis and research were done on the pore structure of coal samples both before and after the displacement experiment.

The purpose of the paper is to investigate typical mines in low permeability coal reservoirs in mining regions in the Huainan and Huaibei areas of China. Using self-made CO<sub>2</sub> displacement experiment equipment, an experimental examination of CO<sub>2</sub> displacing CH<sub>4</sub> was conducted. By using an experimental setup, the alternations in gas flow during CO<sub>2</sub> displacement were observed, and the coal-like pore structure before and after CO<sub>2</sub> displacement was examined.

## 2. Test Method

### 2.1 Sample Acquisition and Preparation

The No.13 coal seam of LiuZhuang and the No.7 coal seam of QiDong in Huainan and Huaibei areas of China were used as the main structural coal sources for this study. The results of the basic physical properties analysis of the collected coal samples are demonstrated in Table 1. Liu Zhuang No.13 and Qi Dong No.7 coal seams are located at depths of 763 and 1044 meters, respectively, with moisture contents of 1.25% and 0.8% and mirror grade group reflectance of 0.7252% and 0.7558%.

Table 1. Basic physical properties of coal samples

Industry analysis of coal samples		
Name of sample	13 coal seam of LiuZhuang	7 coal seam of QiDong
Type of coal	Gas coal	Fat coal
Depth of sampling	763m	1 044m
Moisture content( $M_{ad}$ )	1.25%	0.88%
Volatile matter( $V_{daf}$ )	39.34%	38.59%
Fixed carbon( $FC_{ad}$ )	39.81%	49.51%
Ash content( $A_{ad}$ )	19.60%	11.02%
Average True relative density ( $g/cm^3$ )	1.36	1.45
Vitrinite reflectance( $R_o$ )	0.7252%	0.7558%

### 2.2 Experimental Apparatus

The schematic diagram of the experimental protocol of this study is illustrated in figure 1. To ensure that the pressure at the inlet meets the experimental requirements, gas booster pumps, and air compressors are used to pressurize the injected gas. A pressure-reducing valve regulates the pressure at the inlet, and a pressure-return valve controls the pressure at the outlet. To maintain temperature stability, a thermostat heats the sample holder. Pressure sensors are positioned at the inlet, outlet and both sides of the holder to monitor the inlet, outlet, perimeter and axial pressure as well as to transfer the collected pressure data to a computer. The rubber tube for gas conduction is linked to the bottle with clarified lime water,

which is used to check the gas. The position of it is at the end of the pipe, where the gas flow meter continuously checks the gas flow at the outlet end.

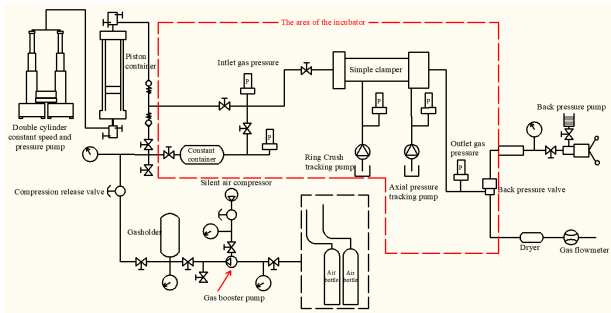


Figure 1. Experimental flow diagram

### 2.3 Experimental Method

The studies tested the change in permeability and the degree of expansion and contraction of coal samples before and after CO<sub>2</sub> displacement under conditions of constant temperature, varied gas injection pressure, and varying surrounding pressure.

#### 2.3.1 Determination of Gas Permeability in Single Component during Pressure Change.

The temperature for the experiment is 36 °C. Pressure conditions at the inlet are 2MPa, 3MPa, 4MPa and 5MPa. The experimental samples were 50mm x 100mm cylindrical samples from the coal seam of LiuZhuang No.13. N<sub>2</sub> and CO<sub>2</sub> are used as the experimental gas (Considering the safety of the experiment. N<sub>2</sub>, which has similar properties, was used instead of CH<sub>4</sub> for the experiments). The specific steps of the experiment are as follows:

- (1) The coal pillar sample is dried and fixed to one end of the holder with adhesive tape. The coal pillar is then covered to enhance axial pressure and placed into the holder with the rubber cylinder. Ultimately, vacuum extraction and closure detection were performed.
- (2) To obtain data continuously until the current gas pressure at the inlet is complete, preload the axial and surrounding pressure to 4 MPa, control the loading rate at roughly 0.2 MPa/s, adjust the N<sub>2</sub> gas pressure at the inlet to 2 MPa, and keep the axial pressure tracking pump and surrounding pressure tracking pump always higher than the gas pressure at the inlet by 2 MPa. The pressure was then changed to 3 MPa, 4 MPa, and 5 MPa. When the experiment is complete, the vacuum is removed from the holder and the pipework and substituted with CO<sub>2</sub> gas to repeat the experiment using the same procedures as before.

#### 2.3.2 Simulating CO<sub>2</sub> Displacement under Deep Buried Conditions

In order to simulate the stratum conditions at an embedded depth of 900m, the simulated experimental temperature was set to 36 °C, the gas pressure at the inlet end was set at 9 MPa, the effective stress of the coal pillar was set at 2 MPa, and the samples were taken from the

coal pillar of the LiuZhuang No.13 coal seam and the QiDong No.7 coal seam in accordance with the progressive gradients of temperature and pressure of the coal strata. Below is the particular experimental protocol: (1) The coal pillar with strain gauges attached were loaded into the holder with heat-shrinkable tubes, and the seal was examined by He. The thermostat was set to a temperature of 36 °C. The next experiment was launched following the stabilization of the temperature.

(2) Vacuum each experimental module for at least an hour, as well as the holder and the pipes.

(3) The N<sub>2</sub> gas pressure at the inlet was set and regulated at 9 MPa. Once the flow rate had stabilized, the gas pressure at the outlet was changed to detect and monitor the gas flow rate at the tail end. Based on the recorded data for the gas input and outlet pressure and flow rate, the N<sub>2</sub> gas permeability of the coal pillar was then estimated.

(4) To guarantee that the coal sample adsorbs N<sub>2</sub> for more than 24 hours, close the gas valve at the outlet end and regulate the N<sub>2</sub> gas pressure at the intake. According to the adsorption equilibrium standard, stable adsorption of a coal pillar is defined as a pressure change in the gas buffer tank within two hours of less than 0.01 MPa.

(5) CO<sub>2</sub> is loaded and injected at a particular pressure, typically 0.5 MPa above the N<sub>2</sub> injection pressure, following vacuum treatment of the pipeline and storage tank. Record the permeability change and stress strain during this process, and make sure that CO<sub>2</sub> enters the coal sample to complete adsorption and desorption.

## 3. Results and Discussion

### 3.1 Changes in Permeability of Single Component Gases

The calculation formula of penetration is as follows [21-24]:

$$k_{ge} = \frac{2p_d q_{ge} \mu_g h}{A(p_u^2 - p_d^2)} \times 100 \quad (1)$$

where  $k_{ge}$  is permeability (mD),  $p_u$  and  $p_d$  are the pressures upstream and downstream of the sample (MPa),  $q_{ge}$  is velocity (cm<sup>3</sup> /s),  $\mu_g$  is viscosity (mPa · s),  $h$  is the sample length (cm), and  $A$  is the sample cross-sectional area (cm<sup>2</sup>). It can be observed from figure 3 that the gas permeability usually grows as the gas pressure at the inlet rises from 2MPa to 5MPa. The enlargement of pore fissures in the coal pillar brought on by the rise in gas pressure at the entry may be the cause of the growing permeability. Simultaneously, the increase in porosity between 2MPa and 3MPa is more noticeable. N<sub>2</sub> and CO<sub>2</sub> have a permeability of between 0.0006 and 0.0007mD, with CO<sub>2</sub> having a considerably lesser permeability than N<sub>2</sub>. The explanation could be that the coal matrix absorbs CO<sub>2</sub> more readily and that the impact of matrix expansion on pore fracture compression is more pronounced, leading to reduced permeability.

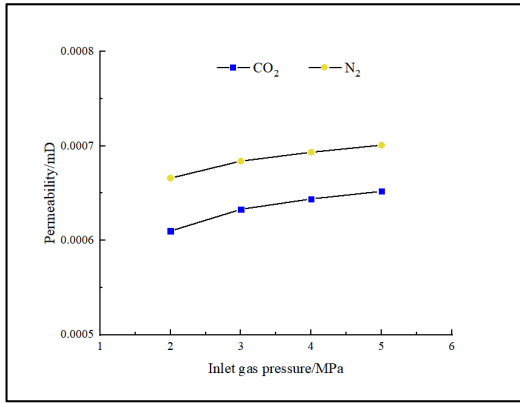
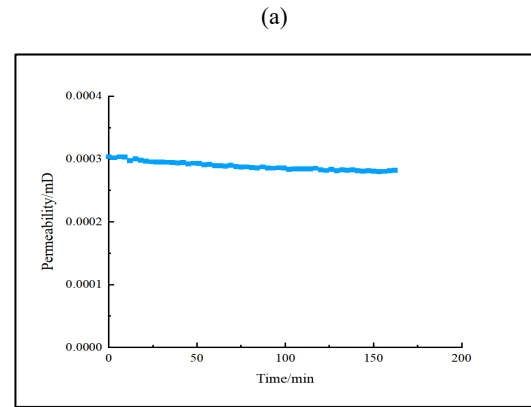
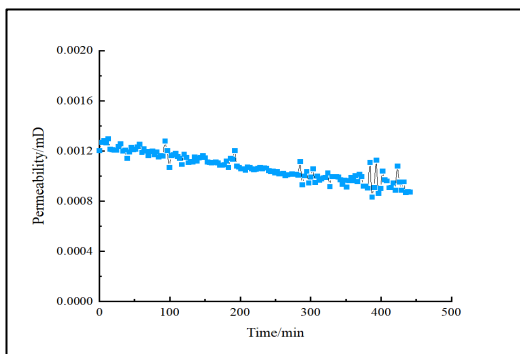


Figure 2. Changes in CO<sub>2</sub> and N<sub>2</sub> permeability with pressure

### 3.2 Characteristics of Gas Permeability under Simulated Reservoir Condition

#### 3.2.1 Original Penetration

As shown in figure 3, the flow rate of N<sub>2</sub> gas at 9MPa injection pressure is calculated and the point line diagram of coal permeability which changes with time is obtained by employing Darcy's Law. The computed samples of Liu Zhuang had total permeability ranging from 0.0008mD to 0.0012mD (1mD=9.869\*10<sup>-4</sup>μm<sup>2</sup>), whereas Qidong's was around 0.0003mD. At the temperature and pressure conditions of 36°C and 9 MPa, both samples showed low permeability. Additionally, when the N<sub>2</sub> transit duration increased, the permeability continued to decrease. Generally speaking, there are several variables that impact how permeable coal seams are. While geological structure, stress condition, and other factors all have an impact on permeability, coal seam pores and fissures have the greatest influence. In the research area, low-permeability coal from China's Huainan and Huaibei mining regions was chosen, and the sample and permeability test was chosen to avoid the evident fracture area of the sample. It results in a significantly low permeability of the sample. The pore structure of the coal will also be compressed by the effective stress during the permeability test, which will lower the permeability. The coal matrix, on the other hand, has the ability to expand during gas adsorption and contract during gas desorption. The volume expansion of the experiment, which was brought on by the coal matrix's adsorption of N<sub>2</sub> gas, constricted the coal's linked pore fissures and led to a steady drop in coal permeability with N<sub>2</sub> injection.



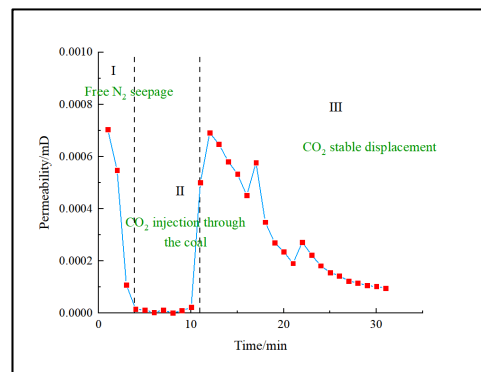
(a)

(b)

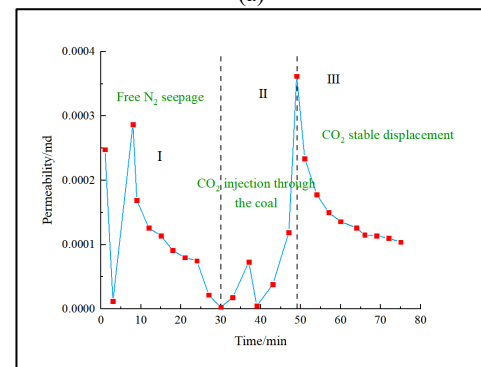
Figure 3. Variation of N<sub>2</sub> permeability of samples in the study area with time (a: LiuZhuang No.13 Coal; b: QiDong No.7 Coal)

#### 3.2.2 Changes in Permeability of CO<sub>2</sub> Displacement.

When adsorbed N<sub>2</sub> had saturated the coal pillar, CO<sub>2</sub> was utilized to displace N<sub>2</sub> from the coal using a repelling pressure that was 0.5MPa greater than the fluid pressure of the coal pillar. Figure 4 depicts the estimated variation in coal pillar permeability over time throughout the displacement process. It is evident that both samples exhibit a comparable fluctuation in permeability. Based on the features of the sample permeability changes, the CO<sub>2</sub> displacement process may be separated into three stages:



(a)



(b)

Figure 4. Change of CO<sub>2</sub> permeability over time in study area (a: Liu Zhuang No.13 coal; b: Qidong No.7 coal)



①Stage I: Free N<sub>2</sub> seepage stage. This stage occurs when the free nitrogen gas in the coal pillar connecting the fissure is first detected to flow out by the tail end and the CO<sub>2</sub> gas at the intake end just begins to be injected. The gas flow rate at the outlet end and the permeability of the recorded data point both steadily decrease as a result of the slow outflow of free nitrogen in the coal pillar's connecting pore fissure. The measured permeability of the coal pillar is now inaccurate and only accurately measures the size of the gas flow rate at the output end. According to the comparison between LiuZhuang No.13 and QiDong No.7 samples in Figure 4, the permeability of LiuZhuang decreases at a faster rate. It is obvious that the LiuZhuang mine sample has higher a pore connection and faster free gas discharge.

②Stage II: Stage of CO<sub>2</sub> injection through the coal. During this phase, CO<sub>2</sub> slowly permeates the coal pillar and enters the coal matrix, and the permeability will exhibit an upward trend. CO<sub>2</sub> initially penetrates the coal pillar's continuous pore-fissure before slowly making its way into the coal matrix, where it competes with the adsorbed N<sub>2</sub> there. The gas flow rate at the end is very low and the permeability measurement value of the coal pillar is comparatively low because it does not enter the coal pillar.

③Stage III: Stage of CO<sub>2</sub> stable displacement. At this point, CO<sub>2</sub> penetrates the coal pillar, and the gas flow rate at the exit end causes the test permeability to gradually drop. CO<sub>2</sub> enters the coal matrix as it is injected to permeate the coal, competing with N<sub>2</sub> for adsorption and promoting N<sub>2</sub> gas desorption. The gas flow rate at the intake end is greater than that at the output end because the coal matrix can adsorb more CO<sub>2</sub> than N<sub>2</sub>. On the other hand, during the displacement process, the coal matrix expands in volume as a result of CO<sub>2</sub> adsorption, which causes the gas permeability to steadily decrease over time.

### 3.2.3 Characteristics of Pore Structure Response after CO<sub>2</sub>-ECBM Process.

#### 3.2.3.1. Strain Characteristics of Coal.

At room temperature, coal is a type of vitreous material with a linked molecular structure system, and it has the properties like brittleness, hardness, and tensile. The initial stress condition of the original coal seam will alter as a result of the CO<sub>2</sub> injection displacement. The desorption of CH<sub>4</sub> and re-adsorption of CO<sub>2</sub> in the coal reservoir will take place concurrently with the injection of CO<sub>2</sub>, causing contraction and expansion of the coal matrix. Accordingly, using the LiuZhuang mine sample as an example, strain monitoring experiments of the coal matrix modeling the CO<sub>2</sub> displacement process are carried out to investigate the strain variations of the coal matrix.

#### (1) Adsorption Strain

As seen in Figure 5, a sample adsorption experiment using N<sub>2</sub> in the coal pillar is carried out while the axial and radial strain of the coal pillar is being measured. After loading the surrounding and axial pressure with the sample and bench-marking the coal substrate, the compression and stretch should be negative and positive, respectively. As can be seen, axial and radial strain is somewhat decreased

and then steadily raised throughout the processes of gas injection and coal substrate adsorption. This is because during the first stage of the N<sub>2</sub> injection to link the coal, axial tension was applied to the coal pillar to compress the coal. The coal matrix then starts to absorb the gas that is expanding as N<sub>2</sub> slowly permeates the coal, gradually increasing the axial and radial strain.

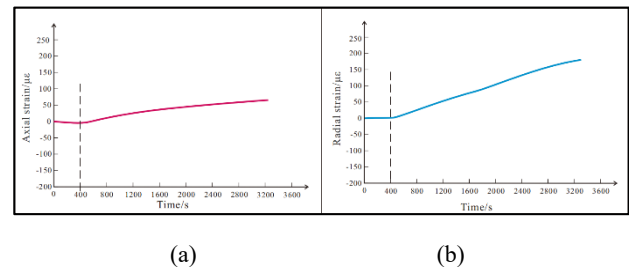


Figure 5. Strain variation with time during adsorption of Liu Zhuang coal sample (a: Axial Strain; b: Radial Strain)

#### (2) Displacement Strain

Once the N<sub>2</sub> adsorption test was finished, CO<sub>2</sub> was introduced into the coal pillar to begin the displacement while the volumetric strain of the coal pillar was monitored. While the effective tension on the coal pillar in the holder remained constant, the adsorption/desorption of the coal matrix was primarily responsible for controlling the strain of the coal matrix. According to the operation flow, the entire experimental procedure may be separated into three stages. The corresponding strains are presented in Fig. 6, and the strain at the start of the CO<sub>2</sub> injection is set as the baseline strain.

①Stage I: Phase of CO<sub>2</sub> injection and adsorption. At this point, CO<sub>2</sub> was fed into the coal pillar to ensure that it was fully in touch with the coal matrix, but the gas valve at the outlet end was left closed to prevent leaks. As more CO<sub>2</sub> is absorbed by the coal matrix than N<sub>2</sub>, this causes a comparatively substantial amount of adsorption expansion, which causes both axial and radial stresses to continuously grow at this time.

②Stage II: Phase of CO<sub>2</sub> displacement and flow. The gas valve at the outlet end is opened at the start of this stage, and the quick flow of gas from the fissure of the coal pillar causes a rapid drop in fluid pressure, which causes significant desorption of gas from the coal matrix and a rapid drop in coal matrix strain. After that, the coal sample's CO<sub>2</sub> gas progressively enters the coal, raising the fluid pressure and resulting in the slow adsorption of the coal matrix. The axial and radial strains of the coal pillar fluctuate unpredictably. The adsorption and expansion of the coal matrix cause a minor rise in the strain of the coal matrix when CO<sub>2</sub> gas is gradually fed into the coal pillar.

③Stage III: Phase of CO<sub>2</sub> stable displacement. The CO<sub>2</sub> adsorption of the coal matrix at the same time displaces the CH<sub>4</sub> output, and the strain of the coal matrix gradually stabilizes.

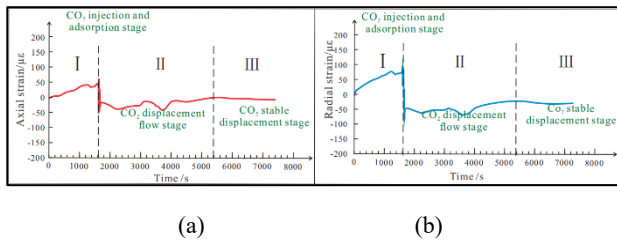


Figure 6. Strain variation with time during Liu Zhuang coal displacement (a: Axial Strain; b: Radial Strain)

### 3.2.3.2. Strain Characteristics of Coal.

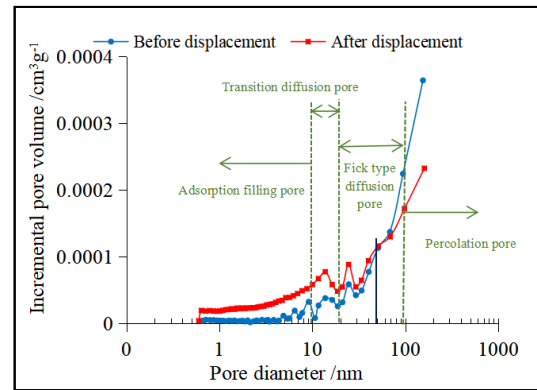
Coal is an example of a typical porous medium with a complicated structure, mostly composed of matrix pores and fracture systems. The high-pressure fluid will enter the coal pore fissure, enlarge it, and improve the coal permeability while simultaneously compressing the coal sample under high-pressure CO<sub>2</sub> injection. On the other hand, during the CO<sub>2</sub> injection to displace N<sub>2</sub>, the coal matrix may potentially alter the pore-fissure structure of the coal. Based on various study objectives and levels of testing accuracy, domestic and international academics have developed numerous criteria for classifying the pore structure of coal (Table 2).

Table 2. Comparison of coal pore size structure classification schemes (Diameter unit: nm)

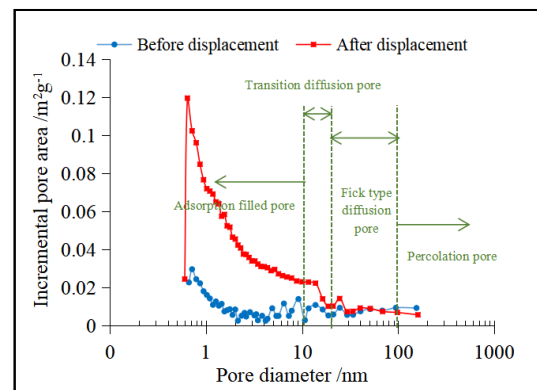
	B. B. Ходот (1961)	Dubin (1966)	IUPAC (1966)	H. Gan (1972)	Coal Research Institute of FuShun (1985)	Sijing Yong et al. (1991)
Micropore	<10	<2	<2	<1.2	<8	<10
Transitional pore	10-100	Transitiona pore	Transitiona pore	Transitiona pore	Transitiona pore	10-50
Mesopore	100-1000	2-20	2-50	1.2-30	8-100	Mesopore 50-750
Macropore	>1000	Macropore	Macropore	Macropore	Macropore	Macropore >750

The process of gas movement during CO<sub>2</sub> displacement in coal seams is the focus of the current investigation. In light of the results of the analysis of the diffusion-percolation characteristics of CH<sub>4</sub> and CO<sub>2</sub> gases in coal and taking into account the opposite diffusion and competitive adsorption of CH<sub>4</sub> and CO<sub>2</sub>, the pores in this study were classified into the following categories: adsorption-filled pores (<10nm), transition diffusion pores (10-20nm), Fick diffusion pores (20-100nm) and percolation pores (>100nm). The most widely used techniques for studying the pore structure of coal are

mercury porosimetry, low-temperature nitrogen adsorption, and CO<sub>2</sub> adsorption. The BET technique is one of them and can measure pores up to 0.35 and 200nm in size, which can measure practically all pore types. Consequently, using a Liuzhuang sample as an example, the structural alterations of the pores and fractures of the coal body before and after the CO<sub>2</sub> displacement treatment were examined in this work using the low-temperature nitrogen adsorption technique.



(a)



(b)

Figure 7. Pore volume changes of LiuZhuang coal sample before and after the experiment of using CO<sub>2</sub> to displace N<sub>2</sub> (a: Pore volume increment; b: Total pore volume)

Pore volume is the total volume of tiny pores within the mass of a porous solid. Each of these crucial factors helps determine the pore fracture structure of coal. Specific surface area is the total area per unit mass of material. Figure 8 compares the findings of the LiuZhuang coal sample's pore volume before and after the experiment in which N<sub>2</sub> was replaced by CO<sub>2</sub>. As can be observed, the displacement resulted in a large increase in the coal's overall pore volume. While the pore volume bigger than 50nm declines, concentrating in some Fick-type diffusion pores and percolation pore sections, the rise in pore volume is primarily seen in the pore size less than 50nm, of which the volume and proportion of adsorption-filled pores (10nm) increase the most.

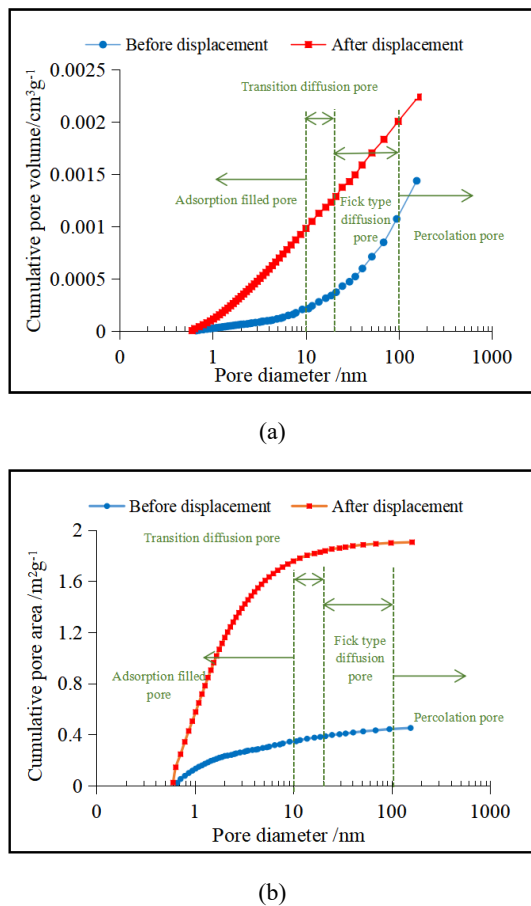


Figure 8. Change of pore specific surface area before and after the experiment of N<sub>2</sub> displacement by CO<sub>2</sub> in low permeability coal seam (a: Increment of pores specific surface area; b: Total specific surface area)

It can be shown in Fig. 8 that the displacement process greatly increased the specific surface area of the micro-pore section of coal samples (approximately 4 times greater after displacement than before displacement) and that the increase is mostly concentrated in the adsorption-filled pore section (< 10nm). This suggests that the CO<sub>2</sub> displacement helps to significantly boost the coal sample's ability to adsorb gas.

Hence, the CO<sub>2</sub> injection procedure will significantly contribute to changing the pores of the coal during CO<sub>2</sub>-ECBM in low-permeability coal seams. Percolation pores primarily regulate changes in coal body permeability, while adsorption-filled and diffusion pores control gas exchange and sequestration in the coal matrix. The expansion of sorption-fill and diffusion pores after CO<sub>2</sub> displacement aids in the complete exchange of CO<sub>2</sub> and CH<sub>4</sub>, increasing the ability of the coal matrix to contain the gas. However, the compression of percolation pores may decrease the permeability of the coal matrix, which would then make it more difficult to inject CO<sub>2</sub>.

#### 4. Conclusion

By conducting the CO<sub>2</sub>-N<sub>2</sub> displacement tests and low-temperature liquid nitrogen adsorption experiment, research the characteristics of gas flow in porous media

and pore structure response characteristics during the CO<sub>2</sub>-ECBM process.

The total N<sub>2</sub> permeability of the Liu Zhuang sample varies between 0.0008mD and 0.0014mD, while the permeability of the Qi Dong sample is around 0.0003mD. When the expansion caused by N<sub>2</sub> adsorption by the coal matrix increases gas injection time, the permeability steadily decreases. Low permeability is a result of the samples' preparation, which avoided apparent fracture zones, and the effective stress of the test, which compressed the pore-fracture structure of the coal.

There are three stages to the CO<sub>2</sub> displacement phase. Free nitrogen exits from the tail end during the free nitrogen stage, and the permeability constantly drops. When there is no penetration, the permeability tends to be lower, but it tends to rise throughout the CO<sub>2</sub> injection penetration stage. In the stage of steady displacement of CO<sub>2</sub>, the gas permeability steadily decreases over time.

At the initial stage of N<sub>2</sub> injection, the axial and radial strain decreased slightly; at the initial stage of CO<sub>2</sub> injection, the axial and radial strain increased gradually; at the stage of continuous CO<sub>2</sub> injection and penetration into the coal, the axial and radial strain fluctuated and increased slightly overall; at the stable stage of CO<sub>2</sub> displacement, the axial and radial strain became stable.

Following the displacement, the total pore volume of the coal dramatically rises, with the majority of the growth occurring in the adsorption-filled pore (pore diameter <10nm). The Fick-type diffusion and permeation pore sections (pore diameter >50nm) are where the majority of the reduction in pore volume is focused. After the displacement, the specific surface area of the pore volume increased four times more than it had previously, with the majority of the increase occurring in the filled pore section (pore diameter <10nm). The CO<sub>2</sub> injection in the CO<sub>2</sub>-ECBM process causes the diffusion and adsorption-filled pores to expand, while the compression of the permeation pores causes a reduction in permeability.

#### References

1. Junlin Liu, Huihu Liu, Kun Zhang, et al. Diffusion characteristics of CO<sub>2</sub> and CH<sub>4</sub> in CO<sub>2</sub>-ECBM process of low permeability coal seam[J/OL]. Coal Science and Technology :1-11[2023-03-30].
2. Busch A, Gensterblum Y. CBM and CO<sub>2</sub>-ECBM related sorption processes in coal: a review[J]. Coal Geol 2011; 87:49e71.
3. Lin J, Ren T, Wang GD, Nencik J. Simulation investigation of N<sub>2</sub>-injection enhanced gas drainage: model development and identification of critical parameters[J]. Nat Gas Sci Eng 2018; 55:30-41.
4. Fan N, Wang JR, Deng CB, et al. Numerical study on enhancing coalbed methane recovery by injecting N<sub>2</sub>/CO<sub>2</sub> mixtures and its geological significance[J]. Energy Sci Eng 2019.
5. Bai G, Zeng XK, Li XM, et al. Influence of carbon dioxide on the adsorption of methane by coal using low-field nuclear magnetic resonance[J]. Energy Fuel 2020;34(5):6113-23.

6. Wenping Jiang, Yongjun Cui. A Discussion on Main Geologic Controlling Factors of CO<sub>2</sub> Sequestration in Deep Coal Seams[J]. *Coal Geology of China*, 2010, 22 (11): 1-6.
7. Lin J, Ren T, Wang GD, et al. Experimental study of the adsorption-induced coal matrix swelling and its impact on ECBM[J]. *Earth Sci* 2017;28(5):917-25.
8. Li Y, Wang Y, Wang J, Pan Z. Variation in permeability during CO<sub>2</sub>-CH<sub>4</sub> displacement in coal seams: Part 1-Experimental insights[J]. *Fuel* 2019;116666.
9. Gang Bai, Jun Su, Zunguo Zhang, Anchang Lan, Xihua Zhou, Fei Gao, Jianbin Zhou, Effect of CO<sub>2</sub> injection on CH<sub>4</sub> desorption rate in poor permeability coal seams: An experimental study[J]. *Energy*, Volume 238, Part A,2022,121674.
10. Di Wu. The reserch on rule of CH<sub>4</sub>/CO<sub>2</sub> seepage-adsorption-desorption and CO<sub>2</sub> displacement CH<sub>4</sub> by injecting CO<sub>2</sub> in residual coal seams under the thermo-mechanical action[D]. LiaoNing Technical University, 2013.
11. Li Y., Tang D., Xu H., et al. Experimental research on coal permeability: The roles of effective stress and gas slippage[J]. *Journal of Natural Gas Science & Engineering*, 2014, 21: 481-488.
12. Zou J., Chen W., Yang D., et al. The impact of effective stress and gas slippage on coal permeability under cyclic loading[J]. *Journal of Natural Gas Science & Engineering*, 2016, 31: 236-248.
13. Yin GZ, Deng BZ, Li MH, et al. Impact of injection pressure on CO<sub>2</sub>-enhanced coalbed methane recovery considering mass transfer between coal fracture and matrix[J]. *Fuel*, 2017; 196: 288-97.
14. Jiajun Xu, Yulong Chen, Chengrong Jiang, et al. Test on carbon dioxide permeability in coal seam[J]. *Mining Safety & Environmental Protection* , 2017, 44(04): 10-13.
15. Wang LG, Wang ZF, Li KZ, Chen HD. Comparison of enhanced coalbed methane recovery by pure N<sub>2</sub> and CO<sub>2</sub> injection: experimental observations and numerical simulation[J]. *Nat Gas Sci Eng* 2015; 23:363-72.
16. Metz B. IPCC Special Report on Carbon Dioxide Capture and Storage[J]. New York: Cambridge University Press; 2005.
17. Li Y, Wang Z, Pan Z, Niu X, Yu Y, Meng S. Pore structure and its fractal dimensions of transitional shale: A cross section from east margin of the Ordos Basin, China[J]. *Fuel* 2019; 241:417-31.
18. Kim HJ, Shi Y, He J, Lee HH, Lee CH. Adsorption characteristics of CO<sub>2</sub> and CH<sub>4</sub> on dry and wet coal from subcritical to supercritical conditions[J]. *Chemical Engineering Journal*, 2011;171(1):45-53.
19. Hemant K, Derek E, Liu J, Pone D, Mathews JP. Permeability evolution of propped artificial fractures in coal on injection of CO<sub>2</sub>[J]. *Petrol Sci Eng* 2015; 133:695-704
20. Li Y, Zhang C, Tang D, Gan Q, Niu X, Shen R. Coal pore size distributions controlled by the coalification process: an experimental study of coals from the Junggar, Ordos, and Qinshui basins in China[J]. *Fuel* 2017; 206:352-63.
21. Izadi G, Wang S, Elsworth D. Permeability evolution of fluid-infiltrated coal containing discrete fractures[J]. *Coal Geol* 2011;85(2):202-11.
22. Skurtveit E, Aker E, Soldal M, Angeli M, Wang Z. Experimental investigation of CO<sub>2</sub> breakthrough and flow mechanism in shale[J]. *Pet Geo Sci* 2012; 18:3-15.
23. Wu Y, Pruess K, Persoff P. Gas flow in porous media with Klinkenberg effects[J]. *Transp Porous Media* 1998; 32:117-37.
24. Kollek JJ. The determination of the permeability of concrete to oxygen by the cembureau method-a recommendation[J]. *Mater Struct* 1989;22(3):225-30.
25. Shuxun Sang, Yanmin Zhu, Jing Zhang, et al. Solid-gas interaction mechanism of coal-adsorbed gas(III)& Physical processes and theoretical models of coal adsorption of gas[J]. *natural gas industry*. 2005, 25(1):4.
26. Yuanping Cheng, Biao Hu. A new pore classification method based on the mechane occurrence and migration characteristics in coal[J]. *Journal of China Coal Society*, 2023, 48(01): 212-225.